IMPROVED MECHANICAL SEAL DESIGN THROUGH MATHEMATICAL MODELLING

by

Richard F. Salant

Manager, Fluid Mechanics and Heat Transfer Department

and

William E. Key

Engineering Specialist

Roy C. Anderson Research Center

Borg-Warner Research Corporation

Des Plaines, Illinois

Richard F. Salant, Manager of the Fluid Mechanics and Heat Transfer Department at the Borg-Warner Research Center, received his B.S. (1963), M.S. (1963) and Sc.D. (1967) in Mechanical Engineering from M.I.T. Prior to joining Borg-Warner in 1972, he held faculty positions at M.I.T. (Associate Professor, Assistant Professor) and the University of California, Berkeley (Assistant Professor). His areas of research have included combustion, theoretical and experimental acoustics, fluid dynamics, heat transfer, and turbomachinery.

William E. Key, Engineering Specialist at the Borg-Warner Research Center, received his B.S. (1964) and M.S. (1967) from the University of California, Berkeley, and did postgraduate work in biophysics at the University of Western Ontario. Prior to joining Borg-Warner in 1974, he held positions at TRW Systems Group (member of the technical staff) and North American Rockwell (Research Engineer). His research has been in the areas of analytical and experimental fluid mechanics, with emphasis on numerical simulation.

ABSTRACT

The mechanical seal manufacturer can now offer the user new seal designs quickly and efficiently, and can respond to troubleshooting requests rapidly, through the use of modern, computerized, seal design techniques.

In particular, a mathematical model of a generalized mechanical seal has been constructed, which incorporates the fluid dynamics of the thin fluid film between the faces and the mechanical and thermal behavior of the various seal components. This model, in the form of a series of interactive computer programs, is used by the seal designer to predict the performance of a given seal design. The designer enters the seal geometry, physical properties of the seal and fluid, and the operating conditions as inputs. The computer programs then determine such seal characteristics as fluid film thickness, power dissipation, torque, leakage rate, deformation characteristics, and temperature distributions.

In developing a new seal, this mathematical model allows the designer to evaluate a large number of alternative designs without the necessity of extensive testing. In troubleshooting an existing seal, the model assists the designer in identifying the sources of problems, and correcting those problems through design changes.

This computerized seal model has been used to analyze a number of seals which have been built and tested. The model predictions agree well with test results.

INTRODUCTION

The design of mechanical seals has remained largely an art since the development of the first mechanical seals in the early 1900s. The seal designer relies primarily on past experience, physical intuition, some very basic calculations, and on a great deal of testing and empirical data. Until recently, he has had few analytical tools with which to work. This has made the development of new seals a time-consuming and expensive process. As the demands of more difficult services, tighter government restrictions, and more sophisticated customers become increasingly stringent, the need for more effective and efficient design methods increases.

Improved seal design methods must be based on physical understanding of the sealing process. However, over the last thirty-five years a great deal of research has been done on mechanical seals, yielding much fundamental understanding, but without having a substantial impact on seal design. This lack of impact stems from the complex geometries of seals. While seal research has been primarily directed towards simplified geometries (which help elucidate the physical phenomena of interest), the results of such research have not been successfully applied to actual commercial seals, because the complex geometries of the latter have not been readily amenable to analysis.

This situation is now changing. The rapid proliferation of computers over the last few years has led to the development of computer programs and hardware which are capable of handling complex seal geometries and which are accessible to the designer. Thus, it is believed it is now timely to apply the basic research results of the last thirty-five years to actual seals.

Such an effort is now underway, and has already achieved a degree of success. The objective of this work is the development of an analytical design tool for mechanical seals, to be used by the average designer, not the researcher. It would be utilized for the analysis of proposed seal designs and alternatives (before they are built), as well as for the troubleshooting of

existing seals. It should be emphasized that this tool is not intended to replace the designer, but rather to serve as a supplement to his other resources.

The approach followed in the present work is to apply existing theories of seal operation to an actual commercial seal, and compare the theoretical predictions with test results. On the basis of such a comparison, the most relevant theory (or theories) is selected and used to construct a mathematical model. The latter is put into a form suitable for use by a designer.

The model is not intended to be completely general and comprehensive, applicable to all types of seals under all conditions. Instead, it is comparatively simple, with many restrictions, but is expandable so that additional features may be added in the future. This model considers complex seal geometries (but they must be axisymmetric), single phase incompressible liquids, steady state operation, and spring-loaded seals (bellows seals are now included, but not discussed in this paper). The model does not consider vibration, misalignment, nor other dynamic effects.

THE SEALING INTERFACE

Conditions at the Interface

The most important portion of a mechanical seal is the interface between the two seal faces. It is here that the actual sealing takes place. Every other part of the seal is designed primarily to provide the proper conditions at this inerface for effective sealing. Hence, the overall design of a seal depends very strongly on the phenomena occuring at the interface.

There are three possible operating conditions at the interface. First, there could be a continuous fluid film over the entire interface, separating the two faces. Under such a condition, there must be a very small, but finite, gap between the faces. Second, there could be mechanical contact between the faces (asperity contact), corresponding to the boundary lubrication regime. Third, there could be a fluid film over part of the interface, and mechanical face contact over the other part.

For many years it was believed that sealing is achieved solely by mechanical contact between the faces. While this may have been the case for early, heavily loaded seals, it is not generally true for modern seals. During operation of the latter, as they experience transients in speed and load from start-up, shut down, and speed and pressure variation, it is likely that all three interface conditions are encountered at various times. Thus, the operation of a modern mechanical seal is quite complex. However, considerable simplification occurs if one considers only the steady state operation of such a seal.

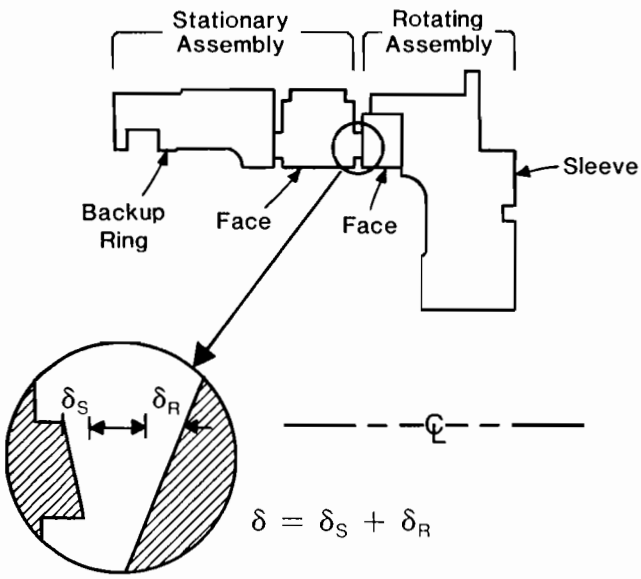

Figure 1. Schematic Drawing of Seal A.

Previous research studies have shown that lightly—to moderately—loaded seals (balance ratios between .5 and 1) in moderately viscous fluids (e.g., water, oil), under steady state conditions, operate with a continuous fluid film at the interface [1]. While this film is extremely thin, 50 to 200 microinches, it is finite. The existence of this film implies that there will always be some leakage. While the leakage may be so small as to be visually undetectable (it may evaporate), it is impossible to eliminate (unless special measures are taken).

To verify the existence of a continuous fluid film for the seals of interest in the present study, a particular "typical" seal has been selected for detailed study. This seal, designated Seal A, is shown in Figure 1. It is a commercially available seal, designed to operate in water at pressures up to 2000 psi and speeds up to 6000 rpm. It has a 6.5 inch balance diameter, a balance ratio of .75, and faces of carbon-graphite and tungsten carbide. Data generated by a series of tests on this seal (in a tester) have been analyzed in three different ways.

First, the torque variations with speed and load have been determined and compared with the known characteristics of continuous fluid films and boundary lubrication interfaces. Such a comparison has shown that Seal A operates with a fluid film. Second, the measured torque values have been used, in conjunction with a simple analytical model of a film, to compute a film thickness (assuming a film exists). This has yielded a film thickness of 87 microinches. Such a value is reasonable since it is larger than the roughness asperity height (10 microinches) and the waviness height (23 microinches) of the faces, but still small enough to limit leakage. Thus, this calculation supports the contention that a fluid film exists. Finally, the wear rate of the carbon-graphite face has been measured and compared with published values for continuous film and boundary lubrication regimes. This has further confirmed the existence of a fluid film. (Details of the above examination of Seal A can be found in [2].) Thus, on the basis of our own measurements, as well as previous investigations, it can be concluded that the seals of interest in the present study operate with a continuous fluid film, under steady state conditions.

Function of the Fluid Film and Design Strategy

It is not surprising that successful mechanical seals operate with a continuous fluid film, since such a film performs an important function: it prevents mechanical contact between the faces. This greatly reduces wear, energy dissipation, and the risk of mechanical and thermal damage. The primary task of the seal designer, then, is to design the seal so that:

a. a stable fluid film is maintained between the faces,

b. the film is thick enough to prevent mechanical contact,

c. the film is thin enough to prevent excessive leakage.

The film thickness is controlled by the position of the floating seal face. As shown in Figure 2, the latter is free to move in the axial direction. It will occupy an equilibrium position which is determined by the forces acting on it, as depicted schematically in Figure 2. Ignoring the spring force (which is insignificant in high pressure seals), it is seen that the net force tending to push the floating face toward the fixed face, the "closing force", is,

$$F_c = \Delta p A_f N_B, \qquad (1)$$

where the balance ration, $N_B = A'/A_f$. (2)

The "opening force", tending to push the floating face away from the fixed face, is produced by the pressure forces within the film and is given by,

$$F_o = \int_{A_f} pdA. \quad (3)$$

F_o will, in general, be a function of the separation between the two faces (the film thickness), because the pressure distribution within the film will depend on film thickness. Thus, the floating face will assume a position (and the film thickness will be fixed) such that,

$$F_o = F_c, \quad (4)$$

and the floating face will be in equilibrium. Therefore, to determine the film thickness it is necessary to understand the pressure distribution within the film.

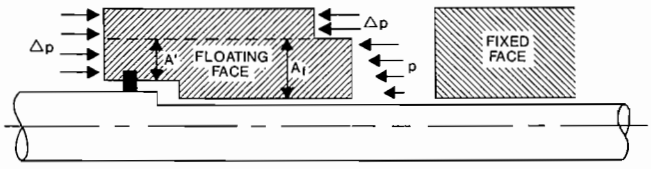

Figure 2. Forces on the Floating Seal Face.

Pressures within the Film

Before the pressure distribution within the film can be computed, it is necessary to adopt a model of the flow field. The simplest such model postulates that the seal faces are perfectly flat, smooth and parallel, producing a uniform fluid film (constant film thickness) with flow through the seal gap from the high pressure side to the low pressure side. For this model, the fluid mechanics equations can be solved in closed form to give an expression for the pressure distribution [3]. In the case in which the seal width is much smaller than the average radius (applicable to most seals), this expression reduces to a linear pressure distribution, i.e., the pressure drops linearly with radial position from the high pressure side to the low pressure. The opening force, as expressed by Equation (3), then becomes,

$$F_o = .5\Delta pA_f, \quad (5)$$

and the force balance, Equation (4), becomes,

$$\Delta pA_fN_B = .5\Delta pA_f. \quad (6)$$

Equation (6) indicates that this simple seal model is unrealistic for two reasons. First, since the opening force is independent of film thickness, Equation (5), this model does not yield a unique film thickness; i.e., the seal should operate with any film thickness. This is incorrect. Second, Equation (6) states that only seals with a balance ratio of .5 can operate with a film. This, too, is incorrect, since seals with balance ratios as high as .85 (or even higher) perform well.

It is clear that the simple seal model, described above, predicts too low an opening force ($.5\Delta pA_f$) to correspond to reality. Thus, there must be some other physical mechanism which produces higher pressures within the film, and, therefore, a higher opening force. Much of the seal research done over the last thirty-five years has dealt with such so-called load support mechanisms. The most important of these are based on effects produced by face roughness, face waviness, misalignment, and/or eccentricity, and face deformation. Each of these features has been shown to increase the pressures within the film. The first three are termed "hydrodynamic mechanisms" because they rely on the rotation of one of the faces to be operable. The last is termed a "hydrostatic mechanism," because it is operable even in the absence of rotation. In the present study, rather than including all of these mechanisms in the mathematical model, it has been decided to first determine the significance of each for the class of seals of interest.

The opening force, F_o, for Seal A has been determined from experimental measurements over a range of operating conditions. The contributions to F_o of each of the four load support mechanisms, discussed above, have been computed from the relevant theoretically derived equations. These calculations have shown that roughness, waviness, and misalignment/eccentricity produce insignificant contributions to the opening force. Only the deformation mechanism is important [2].

It has, therefore, been concluded that for the class of seals of interest, face deformation is the controlling mechanism for load support. Hence, the mathematical model needs only consider the deformation mechanism.

The Deformation Mechanism

Face Deformation

The deformation mechanism is based on the premise that the seal faces are not perfectly flat and parallel with a fluid film of constant thickness, but rather deform to be nonparallel with a variable film thickness. It is this nonuniform film thickness which can give rise to increased pressures within the film, and therefore increased load support.

Figure 1 contains a schematic diagram of Seal A, with a blown-up view of the interface region in which the deformations have been exaggerated. It is assumed that the seal deforms axisymmetrically, so that the faces converge or diverge in the radial direction, going from OD to ID (Figure 1 shows them converging). The amount of deformation of the stationary face is measured by δ_S, and that of the rotating face by δ_R, as shown in the figure. (Note that for Seal A, the stationary face floats in the axial direction and the rotating face floats in the axial direction and the rotating face is fixed). The total deformation is defined as,

$$\delta \equiv \delta_S + \delta_R. \quad (7)$$

A positive value of δ indicates a converging gap (from OD to ID), while a negative value indicates a diverging gap. For convenience, it is assumed that the high pressure side of the seal is at the OD, although this is not necessary to the model.

Since there is a continuous fluid film between the faces, there will be fluid flow from OD to ID, i.e., leakage. Since steady state is assumed, this flow is steady and the flow rate very low since the film thickness is very small. The variation of the film thickness with radius is taken to be of the form,

$$h = Ar^B, \quad (8)$$

where the constants A and B are related to the deformation and other seal parameters by,

$$A \equiv h_i/R_i^B, \quad (9)$$

$$B \equiv \frac{\ell n(1 + \delta/h_i)}{\ell n\alpha}, \quad (10)$$

$$\delta \equiv h_o - h_i \quad (11)$$

B is a measure of the convergence or divergence of the film. A positive B indicates convergence, a negative B divergence, and zero B a uniform film.

Fluid Mechanics Analysis of the Film

The governing fluid mechanics equations for the flow in the converging or diverging fluid film can be solved to yield a closed form expression for the pressure distribution (see Appendix). This distribution is shown in Figure 3. It is seen that converging films produce convex pressure profiles, while diverging films produce concave profiles. The greater the amount of convergence/divergence, the greater the degree of convexity/concavity. Since the opening force is equal to the integral of the pressure over the face, it is clear that converging films produce larger opening forces than a uniform film. In fact, forces large enough to hold in equilibrium seals with balance ratios between .5 and 1 can be generated, depending on the amount of convergence. Conversely, diverging films produce lower opening forces than a uniform film, and correspond to balance ratios between 0 and .5.

A converging film will tend to be stable while a diverging film will tend to be unstable, as is indicated in Figure 3. First, consider a converging film. If there is a sudden increase in film thickness due to an external disturbance (without a change in δ), the amount of convergence (δ/h_i or B) will decrease, and therefore the opening force will decrease. The imbalance between the closing and opening forces will then return the floating face to its original position. Similarly, a sudden decrease in film thickness will result in an increase in opening force, again returning the floating face to its original position. Conversely, for a diverging film, perturbations in the position of the floating face produce force changes which move the floating face away from its equilibrium position, an unstable condition.

Thus, it is clear that a satisfactory seal requires a design which produces a converging film. The remainder of this paper considers only this case.

For a seal with a given geometry, the larger the value of δ/h_i (and therefore B), the greater the degree of convexity of the pressure profile, and the greater the opening force, as is seen in Figure 3. Therefore, for a given seal with a given deformation δ, the floating face will assume an equilibrium position corresponding to a particular value of h_i. The latter will be that value

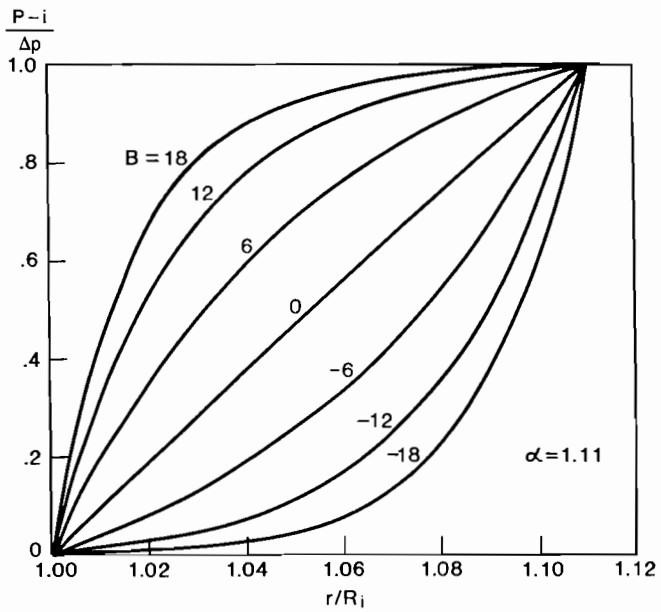

Figure 3. Pressure Distribution in Fluid Film.

which produces a value of δ/h_i (and hence B) corresponding to the particular pressure profile in Figure 3, which yields an opening force exactly equal to the closing force given by Equation (1). Thus, for a given seal, there is a unique film thickness h_i for each operating condition.

For any given seal geometry (N_B and α), one can calculate the closing force (from Equation (1)) and the pressure profile in the film for various values of δ/h_i. Therefore, one can compute the value of δ/h_i necessary for equilibrium. This procedure is contained in the Appendix. It is seen, therefore, that δ/h_i is a function only of the seal geometry, i.e.,

$$\delta/h_i = C_1 (\alpha, N_B) \tag{12}$$

Thus, for a given seal δ/h_i is a constant. This implies that the film thickness is directly proportional to the deformation; i.e., the larger the deformation, the larger the film thickness.

It is therefore seen that to control film thickness, the designer must control the deformation of the seal faces. First, he must design the seal to have positive deformation (converging film). Second, he must design in enough deformation to produce a thick enough film to avoid face contact (h_i must be significantly larger than the asperity height). Note that this contradicts a traditional view held by many seal designers that the ideal seal contains no deformation. Third, the designer must make sure that the deformation is small enough to avoid excessive leakage.

As stated above, one can calculate the equilibrium value of δ/h_i for a particular seal design. Therefore, if one knew the deformation δ, one could easily compute the film thickness. Once the film thickness and deformation are known, all other important characteristics of the seal can be calculated. Equations for the leakage rate, torque and energy dissipation rate, obtained from the solution of the governing fluid mechanics equations, are given in the Appendix. After the energy dissipation rate is obtained, the appropriate heat transfer equations can be solved to yield temperature distributions in the various seal components.

Thus, it is seen that the key to determining the behavior of the seal is the calculation of the seal deformation. This deformation consists of two parts: mechanical deformation and thermal deformation. While the mechanical deformation depends on the pressure loading on the seal (and any other applied forces), the thermal deformation depends on the heat transfer into the seal which, in turn, depends on the energy dissipation rate. Since the latter depends on the film thickness (see Equation (A7) in Appendix), it is not possible to solve for δ, h_i, and all other quantities sequentially. Rather, the deformation and film thickness must be solved for simultaneously.

Deformation Analysis

To determine the deformation δ, not only must the seal faces be considered, but the entire supporting structure must be considered. However, regardless of the structural details, if linear materials are considered, the deformation can be expressed by the following general equation,

$$\delta_{S,R} = K_n K_p \Delta p + K_g K_f H + K_r F_s \tag{13}$$

The constants in the above equation, K's, are termed "influence coefficients." They have fixed values for any particular seal design, and those values are dependent on the structural details. The first term in Equation (13) represents the mechanical deformation, and the second term the thermal deformation. The third term represents the deformation of a face caused by the shear force exerted on that face by its backup ring or holder. However, if the face is always in sliding contact with its backup

ring, as is assumed in the present study, the third term can be absorbed into the first term (since F_s can be expressed in terms of Δp).

Equation (13) could be used to calculate the deformations as functions of Δp and H if one knew the values of the influence coefficients for the particular seal of interest. To obtain the influence coefficients, numerical structural analyses are performed on the entire seal to yield δ_S and δ_R for four particular hypothetical operating conditions. From these calculated values of δ_S and δ_R one can compute the values of the Ks (for the procedure, see [4]). This allows one, then, to compute δ_S and δ_R for any operating condition without further structural analysis.

In the present model, the structural analyses (at the four hypothetical operating conditions) are performed with the commercially available computer program ANSYS.

Each seal face, its holder, and all other components with which it is in contact, are treated together as an assembly. Any number of components in an assembly can be handled. Similarly, any number of assemblies, either rotating or stationary, can be analyzed. This allows analysis of multiple seal systems, such as double and tandem seals. For each mating pair of assemblies, a force balance on the floating face is used to determine the opening force. That, together with the known form of the pressure distribution in the film, yields the latter distribution. The pressure distribution is then inserted into a force balance on the fixed assembly, which yields the restraining force on that assembly. Once all the forces around each assembly are determined, ANSYS is used to perform a finite element analysis of each assembly. It calculates the stresses, strains, and mechanical deformations at each internal grid point (specified by a mesh generating program) within the assembly.

Analysis of thermal deformation requires computation of the temperature distribution in all seal components. The energy dissipated in the film is accounted for by treating the film as a heat source, with strength arbitrarily set at one horsepower (temperature profiles for any heat source strength can be scaled-up). The heat transfer from the film into the faces is apportioned between the faces in inverse proportion to their thermal resistances. Specification of the heat transfer coefficients along the entire periphery of all seal components is done by treating each surface as a rotating or stationary, cylindrical or disc-like surface, and using laboratory-generated coefficients for such surfaces.

Utilizing the above information, ANSYS performs thermal analyses, thermal deformation analyses, and mechanical deformation analyses. Hence, all the influence coefficients can be determined.

Computation of Seal Characteristics

As mentioned previously, for the present model the deformation equation, Equation (13), can be simplified to the form,

$$\delta = C_2\Delta p + C_3 H \tag{14}$$

where C_2 and C_3 are determined from the influence coefficients of the individual faces.

The energy dissipation rate H, as described earlier, is dependent on the film thickness h_{av}, and is given by Equation (A7). By combining Equation (14) with Equations (12) and (A7), one obtains a single algebraic equation for the energy dissipation rate,

$$H = \frac{-C_2\Delta p}{2C_3} + \left[\left(\frac{C_2\Delta p}{2C_3}\right)^2 + \frac{C_1\mu A_f U^2}{C_r C_3(1+.5C_1)}\right]^{1/2} \tag{15}$$

Thus, once the influence coefficients are calculated, H can be computed. Then δ can be calculated from Equation (14), h_i from Equation (12), and Q from Equation (A5).

FORM OF MATHEMATICAL SEAL MODEL

The mathematical seal model, described in the previous sections, has been put in the form of a series of interactive computer programs. These programs are intended to be used by designers, who do not necessarily have detailed knowledge of the contents of the programs. They, therefore, contain many prompts which ask the designer for information and give him instructions, leading him through the sequence. The programs also contain many safeguards and error statements to avoid incorrect and aborted runs. The sequence of operations has been arranged so that modifications and variations of a design can be analyzed without rerunning all computations. An average basic seal analysis takes one to three days (actual time, not computer time), depending on complexity of the design. Once a basic analysis has been performed, analysis of modifications usually requires a few hours (or less). The lagest portions of these times are spent on specification of the problem, interpretation of drawings, and conversion of drawings to data files.

The sequence of operations starts with the designer inputting the seal geometry, which is used to generate finite element meshes for all seal components. Then, the forces and heat loads on the various components are computed. Utilizing this information, ANSYS performs finite element thermal and deformation analyses for the four hypothetical operating conditions required for determination of the influence coefficients. The influence coefficients are then computed, and finally the seal characteristics (e.g., film thickness, leakage rate, etc.) are calculated for various operating conditions. If desired, the programs can be run without the use of influence coefficients, in which case the thermal and deformation analyses are performed at the operating conditions of interest.

When the analysis is completed, the designer is provided with the seal performance characteristics; a typical printout is shown in Figure 4. For each speed, a table is generated giving h_1, δ, h_{av}, T, H, f, Q and face temperature as functions of pressure. The deformation equations for all seal faces are also provided. In addition, as the programs are being run, the designer can call for intermediate information, which is often very useful in evaluating the details of a seal design and in

```
Example Seal:
   -FILM THICKNESS vs PRESSURE & RPM-

LEFT  FACE: DELTA = -0.1216*DP +  43.2*H
RIGHT FACE: DELTA = -0.0246*DP +  54.2*H
 TOTAL: DELTA = -0.1462*DP +  97.4*H

FLUID TEMP = 120 (WATER)
BALANCE = 0.650

SHAFT SPEED = 3500 RPM

  PRESSURE      h1     delta    have     TQ      H        f       QLEAK   TFACE
 psi    bar   muinch   muinch  muinch  lb*ft    hp                cc/min  deg F
 100    6.9   102.7     76.6    141.0   1.40    0.94    0.0112    12.76    142
 200   13.8    96.3     71.8    132.2   1.56    1.04    0.0062    20.24    145
 300   20.7    90.1     67.2    123.7   1.71    1.14    0.0045    24.20    147
 400   27.6    84.5     63.0    116.0   1.87    1.25    0.0037    25.94    150
 500   34.5    79.4     59.2    109.0   2.04    1.36    0.0032    26.28    152
 600   41.4    74.7     55.7    102.6   2.21    1.47    0.0029    25.76    155
 700   48.3    70.4     52.5     96.7   2.39    1.59    0.0027    24.74    158
 800   55.2    65.9     49.2     90.5   2.56    1.71    0.0025    23.10    161


SHAFT SPEED = 4500 RPM

  PRESSURE      h1     delta    have     TQ      H        f       QLEAK   TFACE
 psi    bar   muinch   muinch  muinch  lb*ft    hp                cc/min  deg F
 100    6.9   123.1     91.8    169.0   1.28    1.09    0.0101    25.97    146
 200   13.8   116.6     86.9    160.0   1.39    1.19    0.0055    42.67    148
 300   20.7   110.2     82.2    151.3   1.51    1.29    0.0040    52.72    151
 400   27.6   103.7     77.3    142.4   1.63    1.39    0.0032    57.76    153
 500   34.5    98.1     73.2    134.7   1.75    1.50    0.0028    60.02    156
 600   41.4    93.8     69.4    127.7   1.88    1.61    0.0025    60.25    158
 700   48.3    88.3     65.8    121.2   2.02    1.73    0.0023    59.16    161
 800   55.2    83.9     62.6    115.2   2.15    1.84    0.0021    57.24    164
```

Figure 4. Typical Computer Printout.

deciding on modifications. For example, he can ask for drawings of the deformed components, plots of isotherms, the values of the temperature and displacement at any point, and the coefficients of intermediate equations (e.g. influence coefficients).

EXAMPLES OF MODEL USE

The value of any mathematical model is ultimately dependent on how well it corresponds to reality. The seal model, described in the previous sections, has been used to analyze and troubleshoot many different seal designs. Generally, the results agree well with observed seal behavior. Four examples follow.

Seal A

Seal A, shown in Figure 1, has been described earlier. It is a commercial seal, and many years of experience have shown it to be very well-behaved, exhibiting little leakage and good stability. A unique feature of this seal is its ability to perform just as well at the upper end of its pressure range (2000 psi) as at the lower end.

The mathematical seal model has been used to compute the performance characteristics of this seal over a range of pressure and speed. Figure 5 shows computed curves of the friction coefficient f versus the duty parameter G (a measure of speed and load). Also shown in Figure 5 are experimental points, which have been obtained by running this seal in a tester. It is seen that the agreement between the model predictions and the experimental results are quite good.

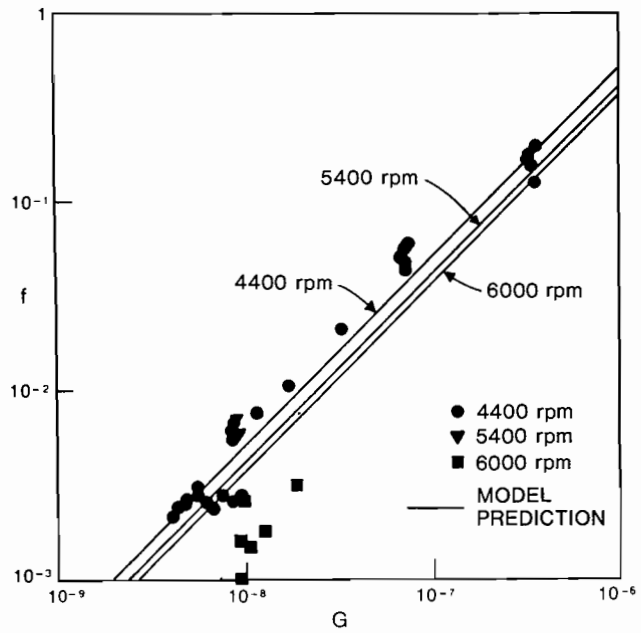

Figure 5. f vs. G, Seal A.

The predicted film thickness is plotted as a function of speed in Figure 6. For the practical operating range (1800-6000 rpm), the model predicts an average film thickness of 45 to 140 microinches. In comparison to the roughness and waviness heights of the faces, these thicknesses are large enough to prevent face contact, but still small enough to prevent excessive leakage. Thus, these results agree with the experienced good behavior of this seal.

The mathematical seal model also predicts the film thickness to be substantially independent of pressure (as implied in Figure 6). This agrees with the experimental observation that the seal performs in a similar manner over its entire pressure range. The reason for this insensitivity to pressure can be seen from the deformation equations generated by the model,

$$\begin{aligned} \delta_S &= -.0664\Delta p + 14.38H \\ \delta_R &= .0716\Delta p + 28.55H \\ \delta &= .0052\Delta p + 42.93H \end{aligned} \quad (16)$$

(In the above equations, δ is in microinches, Δp in psi, H in horsepower).

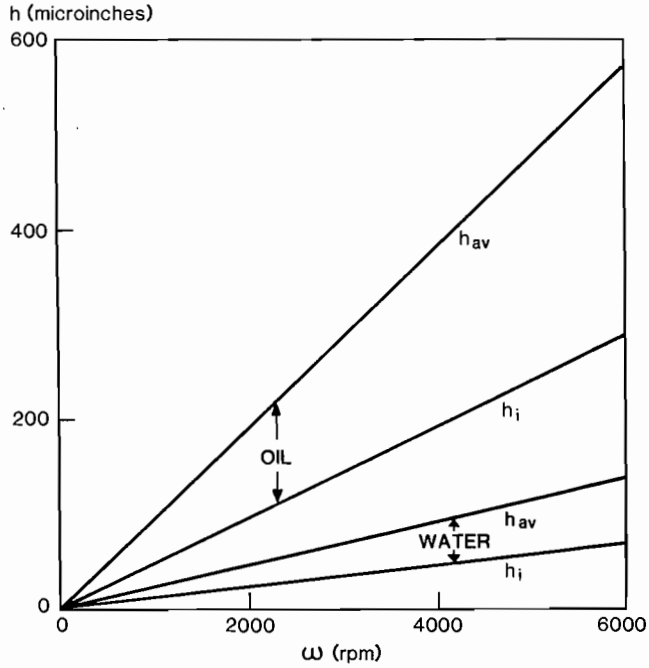

Figure 6. h vs. ω, Seal A.

These equations show that while both seal faces undergo mechanical deformation, which is pressure dependent, such deformation is negative for the stationary face, positive for the rotating face, and both are of nearly the same magnitude. Thus, the two mechanical deformations cancel each other, and do not affect the film. This can be further seen from Figures 7 and 8, which show the deformed shapes of the faces predicted by the model, under pressure loading alone (no thermal loading). Note that the broken lines on the figures represent the undeformed shapes, and the deformations are exaggerated for clarity.

Seal A performs well with water, for which it has been designed. However, if used with oil it leaks excessively, which agrees with the model predictions. Film thicknesses with oil are substantially larger than those with water, as shown in Figure 6. This is because the energy dissipation rate with oil is higher (due to the higher viscosity), leading to larger thermal deformations, and therefore a thicker film. Since the leakage rate varies with the cube of the film thickness, and only inversely with viscosity, it will be much larger with oil.

Seals B and C

In contrast to Seal A, Seals B and C are known to have design effects. They are preliminary designs for the primary and closure seals in a seal system for pumps in an LNG pipeline. They are shown in Figure 9, have balance diameters of 6.5 inches, balance ratios of .82, and tungsten carbide and carbon-graphite faces. Their operating point is 800 psi and 5000 rpm.

Test seals built according to these designs have performed unsatisfactorily, experiencing severe wear. Hence, it was necessary to redesign these seals to achieve satisfactory operation. However, the preliminary designs (Figure 9) serve as a good test case for the mathematical model.

Model predictions of film thickness as a function of speed are shown in Figure 10. In contrast to Seal A, the film thicknesses are pressure dependent, decreasing with increasing pressure. At the operating point, the film thicknesses are 2.4 microinches and .5 microinches. Since these are significantly smaller than the asperity height of 10 microinches, it is clear there will be mechanical contact between the faces, and continuous films cannot be maintained. This is in agreement with the known behavior of these seals.

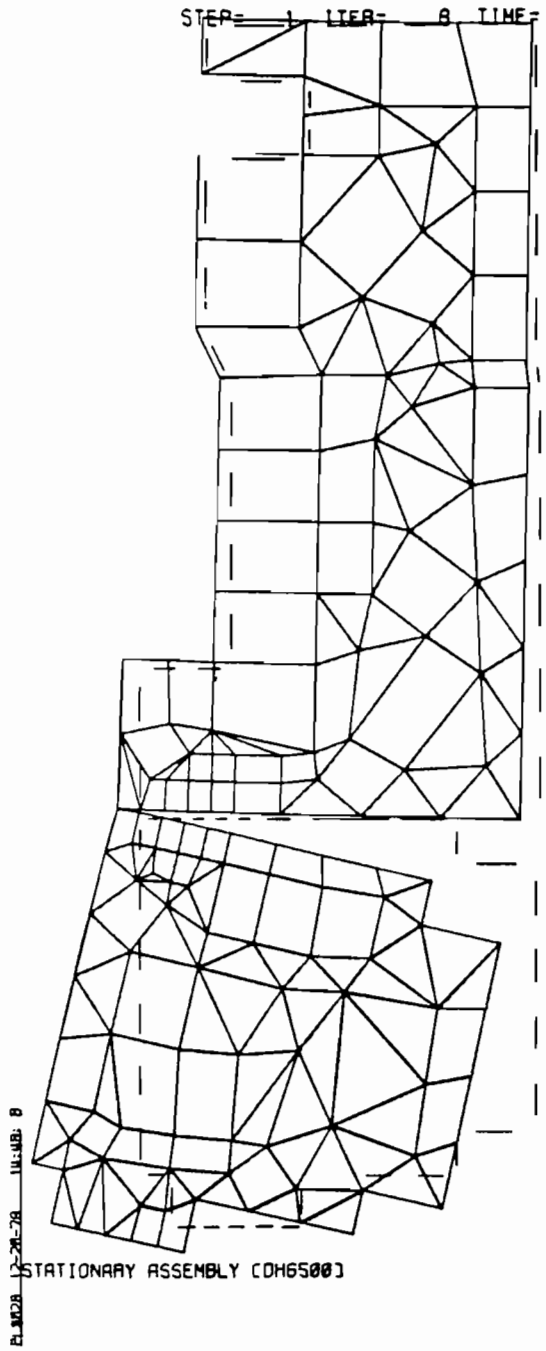

Figure 7. Deformation of Stationary Assembly, Seal A.

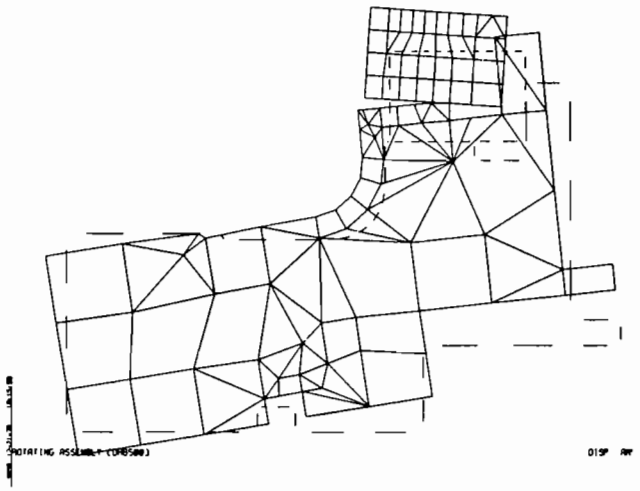

Figure 8. Deformation of Rotating Assembly, Seal A.

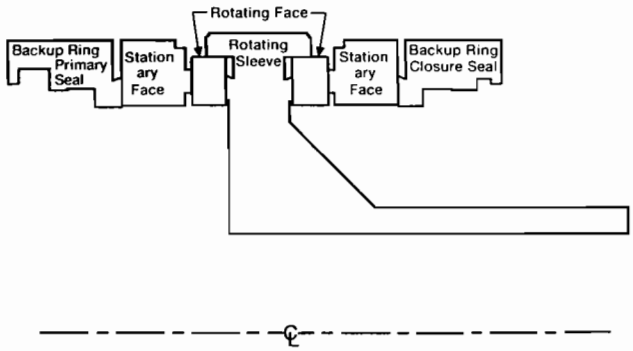

Figure 9. Schematic Drawing of Seals B and C.

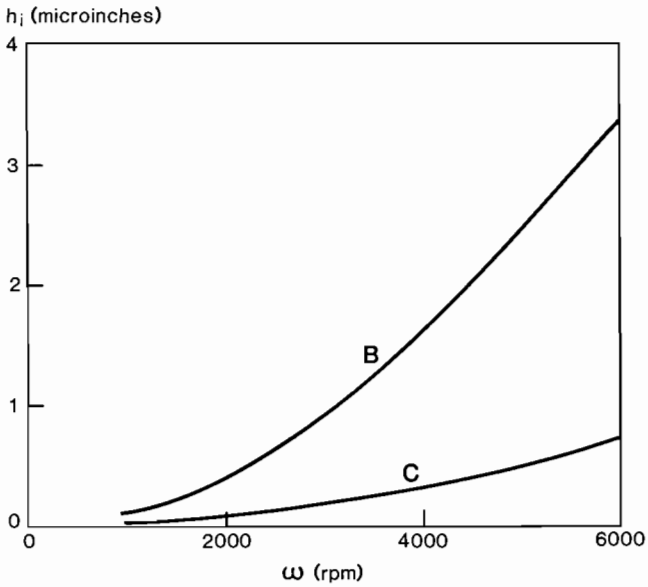

Figure 10. h_i vs. ω, Seals B and C.

The predicted deformation equations reveal the reason for the breakdown of the films.

Seal B

$$\delta = -.1280\Delta p + 10.2771H \quad (17)$$

Seal C

$$\delta = -.1276\Delta p + 1.8404H \quad (18)$$

Comparing Equations (17) and (18) with the equivalent expression for Seal A, Equation (16) indicates that Seals B and C experience too much negative mechanical deformation and not enough positive thermal deformation to maintain a film.

Seal D

Seal D illustrates how very subtle changes in geometry can produce large changes in seal performance. This seal, shown in Figure 11, has been designed for use in boiler feedwater pumps. It has a 6.5 inch balance diameter, .65 balance ratio, and tungsten carbide and carbon-graphite faces. Its operating point is 580 psi and 4500 rpm.

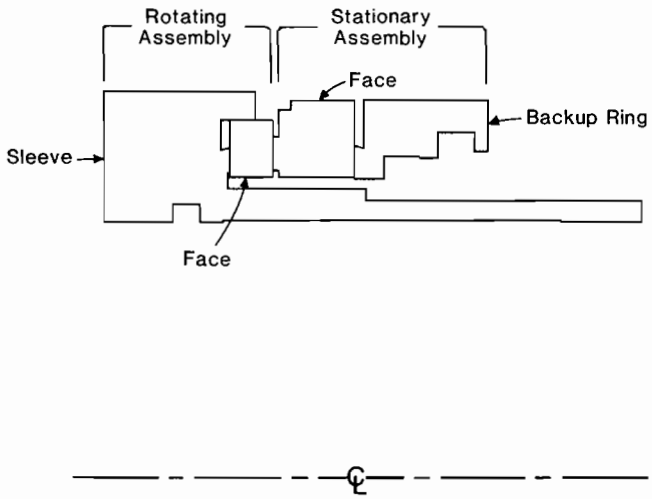

Figure 11. Schematic Drawing of Seals B and C.

In actual use, this seal has experienced a number of structural failures of the tungsten face. To determine if this is due to a design flaw, a complete analysis has been performed. The predicted film thicknesses, shown in Figure 12, indicate that the seal should operate at its design point with a continuous fluid film. No design defect has been found. Subsequently, it was determined that the seal failures were related to water quality and the formation of mineral deposits. When water quality was improved, the seal performed well, confirming the model predictions.

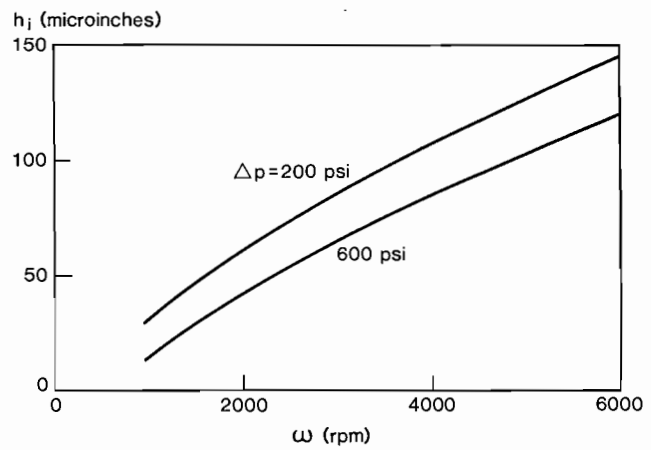

Figure 12. h_i vs. ω, Seal D.

However, tests have also shown that this seal requires a very high starting torque. In a tester, the motor cannot be started while the system is fully pressurized. The reason for this can be seen from the predicted deformation equations.

$$\delta = -.1362\Delta p + 43.4H$$
$$\delta = -.0284\Delta p + 51.6H$$
$$\delta = -.1646\Delta p + 95.0H \quad (19)$$

Equation (19), together with Figure 12, indicates that although there is significant negative mechanical deformation, under steady conditions there is sufficient positive thermal deformation to overcome the mechanical deformation and produce a film. However, at start-up there is virtually no thermal deformation and the seal gap is diverging, resulting in mechanical contact and high torque.

To reduce the starting torque, the seal design has been modified to produce positive mechanical deformation, as shown in Figure 13. A small cutout has been made in the stationary face, and two shoulders in the rotating face holder have been moved. The large effect produced by the latter change can be seen in Figures 14 and 15 which contain deformation shapes generated by the mathematical model. The deformation equations for the modified design are,

Figure 13. Schematic Drawing of Modified Seal D.

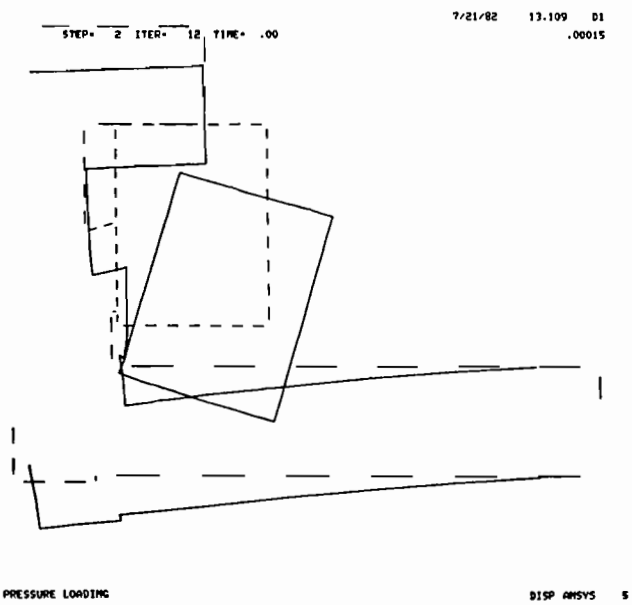

Figure 14. Deformation of Rotating Face, Seal D.

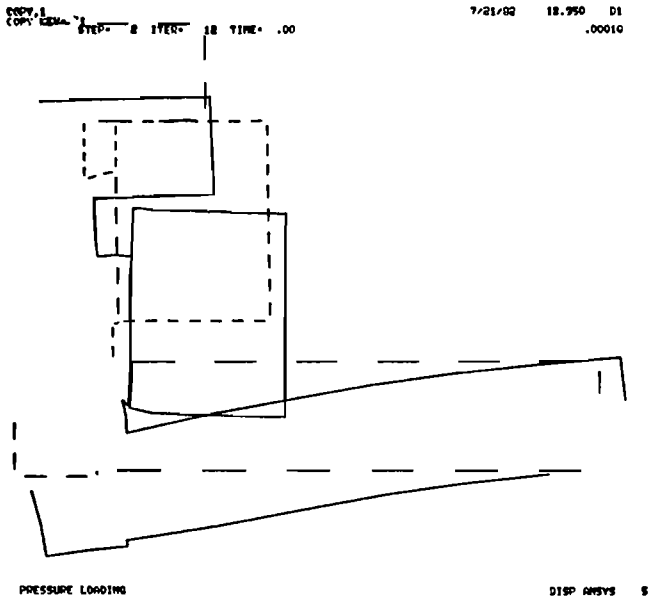

Figure 15. Deformation of Rotating Face, Modified Seal D.

$$\delta_S = .0295\Delta p + 47.1H$$
$$\delta_R = .0061\Delta p + 47.5H$$
$$\delta = .0356\Delta p + 94.6H \qquad (20)$$

Thus, it is clear that the goal of positive mechanical deformation has been achieved. This has been confirmed by tests on the modified design; in fact, the starting torque is so low that the shaft of the tester can be turned by hand with the system fully pressurized.

CONCLUSIONS

From the results reported above, it can be concluded that mathematical modelling provides the designer with a quantitative analytical tool which can be used to predict the performance of prospective seal designs. It is easy to use and yields results quickly. Such quantities as film thickness, face deformation, torque, leakage, and face temperature can be estimated before a seal is built. Experimental results for a number of seals have agreed well with model predictions. While the model developed thus far is not completely general, it has proved extremely useful, and is now routinely utilized for seal evaluation, and as a guide for planning seal test programs.

NOMENCLATURE

A	Constant defined by Equation (8)
A_f	face area
A′	area defined by Figure 2
B	constant defined by Equation (10)
C_1	function of α and N_B defined by Equations (A2)-(A4)
C_2, C_3	coefficients defined by Equation (14)
C_r	correction factor to account for surface roughness, computed using equation from [5]
f	friction factor
F_c	closing force on floating seal face
F_o	opening force on floating seal face
G	duty parameter, $\mu U(R_o-R_i)/F_c$
h	film thickness
h_{av}	average film thickness
h_i	film thickness at ID
h_o	film thickness at OD
H	energy dissipation rate
K_f, K_g, K_n, K_p, K_r	influence coefficients
N_B	balance ratio
N_w	function defined by Equation (A3)
p	pressure
p_i	pressure at ID
Q	leakage flow rate
r	radial coordinate
R_b	balance radius
R_i	inner radius
R_o	outer radius
T	torque
U	average face speed
α	ratio of outer radius to inner radius
Δp	pressure drop across seal
δ	deformation of seal
δ_R	deformation of rotating face
δ_S	deformation of stationary face
ω	angular speed

APPENDIX

Reynolds equation can be solved for flow in the converging or diverging film of Equation (8), to yield the pressure distribution,

$$\frac{p - p_i}{\Delta p} = \frac{1 - (R_i/r)^{3B}}{1 - \alpha^{-3B}} \qquad \text{For } B \neq 0$$
$$= \frac{\ell n\,(R_i/r)}{\ell n\,(1/\alpha)} \qquad \text{For } B = 0 \qquad (A1)$$

Inserting Equation (A1) into Equation (3) and using Equations (4) and (1) results in,

$$N_w = 1/2\,(\alpha^2 - 1)N_B \qquad (A2)$$

where,

$$N_w \equiv \frac{(\alpha^2 - 1)/2 - (\alpha^{2-3B} - 1)/(2 - 3B)}{(1 - \alpha^{-3B})} \qquad \text{For } B \neq 0$$
$$\equiv \frac{(\alpha^2/2)\,\ell n\,\alpha - (\alpha^2 - 1)/4}{\ell n\,\alpha} \qquad \text{For } B = 0 \qquad (A3)$$

From Equation (8) it is seen,

$$\delta/h_i = C_1\,(\alpha, N_B) \qquad (A4)$$

From the solution of Reynolds equation,

$$Q = \left(\frac{\Delta p}{1 - \alpha^{-3B}}\right) \frac{C_r \pi B h_i^3}{2\mu} \qquad (A5)$$

$$T = \frac{\mu A_f U R_b}{C_r h_{av}} \quad \text{(A6)}$$

$$H = \frac{\mu A_f U^2}{C_r h_{av}} \quad \text{(A7)}$$

where

$$h_{av} \equiv h_i + \delta/2 \quad \text{(A8)}$$

REFERENCES

1. Nau, B. S., "Hydronamic Lubrication in Face Seals," *In* Proc. 3rd International Conference on Fluid Dealing, Cranfield, U.K., BHRA Fluid Engineering, (1967).
2. Salant, R. F. and Key, W. E., "Development of an Analytical Model for Use in Mechanical Seal Design," *In* Proc. 10th International Conference on Fluid Sealing, Cranfield, U.K., BHRA Fluid Engineering, (1984).
3. Metcalfe, R., "A Fluid Mechanical Analysis of Axisymmetrical face Seals on the Basis of Constant Viscosity, Laminar Flow," Report AECL-4073, Chalk River, Ontaria, Atomic Energy of Canada Limited. (1971).
4. Metcalfe, R., "End-Face Seal Deflection Effects—The Problems of Two-Component Stationary or Rotating Assemblies," ASLE Trans., *23*, (4), pp. 393-399 (1980).
5. Assam, M. I. S. and Dullien, F. A. L., "Flow in Tubes with Periodic Step Changes in Diameter: A Numerical Solution," Chemical Engineering Science, *32* pp. 1445-1455. (1977).

ACKNOWLEDGEMENT

The contributions of the personnel of Borg-Warner Mechanical Seals to this work are gratefully acknowledged.